Optica Applicata, Vol. XXXVI, No. 4, 2006

Spectroscopy of Cd_2 and Zn_2 molecules in free-jet supersonic beams: experimental and theoretical studies

MAREK RUSZCZAK[1], MARCIN STROJECKI[1], MAREK KROŚNICKI[2,3], MICHAŁ ŁUKOMSKI[1], JAROSŁAW KOPERSKI[1*]

[1]Marian Smoluchowski Institute of Physics, Jagiellonian University, Reymonta 4, 30-059 Kraków, Poland

[2]Institut für Theoretische Chemie, Universität Stuttgart, Pfaffenwaldring 55, 70569 Stuttgart, Germany

[3]Institute of Theoretical Physics and Astrophysics, University of Gdańsk, Wita Stwosza 57, 80-952 Gdańsk, Poland

[*]Corresponding author: J. Koperski, ufkopers@cyf-kr.edu.pl

A method of supersonic beam combined with techniques of laser spectroscopy and simulations of spectra were employed to study interatomic potentials of Cd_2 and Zn_2 molecules. Total laser induced fluorescence was recorded after an excitation of Cd_2 using laser radiation in the range of 2200–2260 Å. The observed structures are interpreted as due to the transitions from $\upsilon'' = 0$ in the ground $X^1 0_g^+$ state to vibrational levels below the potential barrier of the $^1 1_u(5^1P_1)$ electronic state. Studies of Zn_2 consisted of simulations of excitation and fluorescence spectra recorded at the $^1 0_u^+(4^1P_1)$–$X^1 0_g^+$ transition. In the simulations, both isotopic and rotational structures were taken into account.

Keywords: cadmium dimer, zinc dimer, potential energy curves, *ab initio* potentials, excitation spectra, fluorescence spectra, van der Waals molecules, supersonic free-jet beam.

1. Introduction

First laser excitation spectrum recorded at the $^3 0_u^+(5^3P_1) \leftarrow X^1 0_g^+$ transition in Cd_2 produced in supersonic beam was reported by KOWALSKI *et al.* [1]. The same transition was further investigated by CZAJKOWSKI *et al.* [2] using similar experimental approach. References [1] and [2] are the only experimental studies of Cd_2 produced in supersonic beams that had been carried out before those of CZAJKOWSKI and KOPERSKI [3], KOPERSKI *et al.* [4], ŁUKOMSKI *et al.* [5], ŁUKOMSKI and KOPERSKI [6] and ŁUKOMSKI *et al.* [7]. They present corrected characterization of the $X^1 0_g^+$-state potential well based on "hot" bands detected in the excitation at the $^3 0_u^+(5^3P_1) \leftarrow X^1 0_g^+$

transition [3], characterization of the $^3 1_u(5^3P_2)$ [4], $^1 0_u^+(5^1P_1)$ [5, 6], $^3 1_u(5^3P_1)$ [7] and repulsive part of the $X^1 0_g^+$-state [5] potentials. The higher-lying $^1 1_u(5^1P_1)$, $^3 1_u(6^3S_1)$ and $^1 0_u^+(6^1S_0)$ electronic-energy states (see Fig. 1**a**) have never been studied using a direct laser-excitation form the $X^1 0_g^+$-state. Out of the excited electronic states of Zn_2, the $^3 0_u^+$-state correlated with the 4^3P_1 atomic asymptote was the only one to be investigated in the supersonic beam [8, 9].

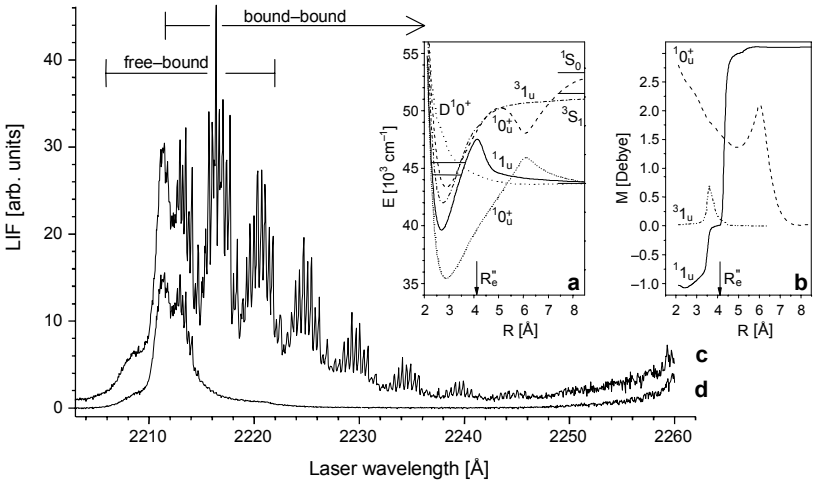

Fig. 1. Interatomic potentials of Cd_2 higher-lying excited electronic-energy states ($^1 1_u(5^1P_1)$, $^3 1_u(6^3S_1)$ and $^1 0_u^+(6^1S_0)$ [16]) possibly involved in the transitions from the $\upsilon'' = 0$ of the $X 0_g^+$ state ($E(\upsilon'' = 0) = 0$ cm^{-1} not shown) – **a**. The range of energies in the $^1 1_u$-state well corresponding to the bound ← bound transitions presented in (**c**) is depicted. Also shown are the $^1 0_u^+(5^1P_1)$ state in Cd_2 and $D^1 0^+(5^1P_1)$ state in CdAr that were investigated in refs. [5] and [14], respectively. Electric dipole moments M versus R for the $^1 1_u(5^1P_1) \leftarrow X 0_g^+$, $^3 1_u(6^3S_1) \leftarrow X 0_g^+$ and $^1 0_u^+(6^1S_0) \leftarrow X 0_g^+$ transitions [16] – **b**. Excitation spectra of Cd_2 observed in this study (details in the text) for: the 0–60 ns time interval (LIF mostly from bound ← bound transitions) – **c**, and 60–1200 ns time interval (LIF mostly from photodissociation of Cd_2) – **d**. Regions of the free ← bound and bound ← bound transitions are shown.

In this article, we present experimental and theoretical studies of Cd_2 and Zn_2 molecules, respectively. Concerning the former, the first attempt of detection of laser induced fluorescence (LIF) after an excitation from the $X^1 0_g^+$ to the higher-lying electronic states correlated with the 5^1P_1, 6^3S_1 and 6^1S_0 atomic asymptotes is reported. Considering the Zn_2, simulations comprising calculation of the vibrational energy states and corresponding Frank–Condon factors (F–CF) for the electronic bound ← bound and free ← bound transitions of the $^1 0_u^+(4^1P_1)$–$X^1 0_g^+$ are presented. To simulate the bound ← bound and free ← bound profiles, the LEVEL 7.7 [10] and BCONT 2.2 [11] codes were used, respectively. At the first stage of the study corresponding *ab initio* interatomic potentials were calculated. The calculations were carried out within the MOLPRO suite of *ab initio* programs [12]. Details of these calculations are given elsewhere [9]. The calculated *ab initio* interatomic potentials

were used as input data for both LEVEL 7.7 and BCONT 2.2 programs. Later on, the calculated F–CFs were used and the isotopic and rotational structures of the transition under investigation were determined. Finally, the Lorentzian or Gaussian convolutions were used to obtain the profiles of the excitation and fluorescence spectra.

2. Spectroscopy of Cd_2

2.1. Experimental

The experimental procedure was described in detail elsewhere [5, 7]. Here, only the most important and most relevant modifications applied in the reported study are emphasized. A molecular beam source was built from stainless (oven body) and heat-resistant (nozzle with an orifice) steels. The molecular beam source was heated up to temperatures 900–950 K. The source was filled with Cd (Aldrich, purity 99.999%, natural abundance) and Ar (Linde, purity 99.999%) as a carrier gas at a pressure of 10 bar. The Cd atoms seeded in Ar were injected through the nozzle (200 μm in diameter) into an evacuated expansion chamber. At distances of 5–7 mm from the nozzle orifice the molecules in the beam were irradiated with a dye-laser beam (Coumarine 120 in Methanol). Vibrational temperature in the beam was estimated [13] to be approximately 5–10 K. The dye laser was pumped by a third harmonic output of a Nd^+:YAG laser (Continuum, Powerlite Series 7000). The dye laser frequency was doubled by an Autotracker with BBO (type I) crystal (Radiant Dyes Laser and Accessories). The frequency calibration of the dye laser fundamental output was verified with 1.0 cm^{-1} accuracy against a WA 4500 pulsed wavemeter (Burleigh) and optogalvanic cell with Ar (Sirah Laser- und Plasmatechnik). The spectral line-width of the dye-laser fundamental output was estimated using a Fabry–Perot etalon (FSR 0.66 cm^{-1}) and was determined to be approximately 0.5 cm^{-1}. The laser and molecular beams were crossed under the right angle in a vacuum chamber. The total laser induced fluorescence (LIF) signal emitted perpendicularly to the plane containing both molecular and laser beams was detected by a photomultiplier tube (Electron Tubes 9893QB/350) and recorded with a digital oscilloscope (Tektronix TDS210). To properly discriminate between the two parts of the measured LIF signal, a time-filtration method was applied. In the first time-interval (from 0 to 60 ns relative to the origin of the dye-laser pulse), LIF is dominated by bound ← bound transitions, while in the second time-interval (from 60 ns to 1.2 μs) LIF originates mostly from photodissociation of Cd_2 (as well as the CdAr [14]) molecules. Additionally, the second harmonic intensity measured with a photodiode was used to normalize the recorded LIF. The procedure also decreased the influence of the laser shot-to-shot instability on the measured signal.

2.2. Results and their interpretation

Figure 1**a** shows three $^1 1_u(5^1P_1)$, $^3 1_u(6^3S_1)$ and $^1 0_u^+(6^1S_0)$ excited electronic states in Cd_2 that are possibly involved in the observed spectra. In the same energy range are two other $^1 0_u^+(5^1P_1)$ and $D^1 0^+(5^1P_1)$ states of Cd_2 and CdAr, respectively. They were

investigated in refs. [5] and [14] (note that CdAr is present in the beam because of Ar being used as a carrier gas). Another insert (see Fig. 1**b**) shows an electric dipole moment M plotted *versus* internuclear separation R for the $^1 1_u(5^1P_1) \leftarrow X\,0_g^+$, $^3 1_u(6^3S_1) \leftarrow X\,0_g^+$ and $^1 0_u^+(6^1S_0) \leftarrow X\,0_g^+$ transitions under cosideration. It is apparent that in the vicinity of the R_e'' (*i.e.*, for a maximum of the $\upsilon'' = 0$-level wave function squared) the $M(R)$ is largest for the $^1 0_u^+(6^1S_0) \leftarrow X^1 0_g^+$ transition which at this point of the discussion indicates that, among the three, the transition to the $^1 0_u^+$ state is most probable. Obviously, transitions to the $^1 1_u$ and $^3 1_u$ states are possible as well (see below), a definite answer to this problem has to wait until additional experiments are performed. Figures 1**c** and 1**d** show the excitation spectra recorded within two different time intervals. Trace **c** represents the LIF integrated through the "short" interval (from 0 to 60 ns relatively to the origin of the dye-laser pulse). It is expected that the total bound ← bound fluorescence from the excited Cd_2 molecules appears within this time period [2]. The recorded bound ← bound transitions extend from 2247 to 2212 Å (*i.e.*, from 44820 to 45530 cm^{-1} relatively to $E(\upsilon'' = 0) = 0$ cm^{-1}) and consist of well resolved vibrational components with noticeable isotopic structure. The appreciable isotopic shift (approx. 6 cm^{-1}) provides information that the excitation occurs up to rather high υ' levels (approx. $\upsilon' = 55$–60) in the respective electronic state. Moreover, a Birge–Sponer plot [15] that was made for the recorded vibrational components reveals distinct curvature implying that the excitation occurs close to the dissociation limit. All this suggests that the $^1 1_u$ is the molecular state up to which the excitation occurs (see the range of energies depicted in Fig. 1**a**). Trace **d** represents the LIF integrated through the "long" interval (from 60 to 1200 ns). It is obvious that in this interval a photodissociation of the Cd_2 molecules dominates providing a wide unstructured maximum which corresponds to free ← bound transitions most likely at the outer part of the $^1 1_u$-state potential barrier (see Fig. 1**a**). It is possible to determine the height of the barrier as approx. 1220 cm^{-1} above the 5^1P_1 asymptote. Therefore, the barrier is approx. 2590 cm^{-1} smaller than or similar to that obtained as a result of *ab initio* calculation of ref. [16] or as presented in ref. [5], respectively. In the long-wavelength part, the spectra rise up slightly. This corresponds to the previously analysed [14] free ← bound spectrum recorded for the $D^1 0^+(5^1P_1) \leftarrow X^1 0^+$ transition in CdAr. Concluding, in order to fully interpret the observed features in the spectra of Fig. 1 more experiments are needed. They are undertaken in our laboratory.

3. Theoretical studies of Zn_2

3.1. Excitation spectrum of the $^1 0_u^+(4^1P_1) \leftarrow X^1 0_g^+$ transition

A simulation of the profile of the excitation spectrum of the $^1 0_{u,\,\upsilon'}^+(4^1P_1) \leftarrow X^1 0_{g,\,\upsilon''=0}^+$ transition is shown in Fig. 2. First, using as the input data *ab initio* calculated interatomic potentials and a LEVEL 7.7 code [10] we determined energies and F–CFs for all allowed vibrational transitions. By solving the radial Schrödinger equation for

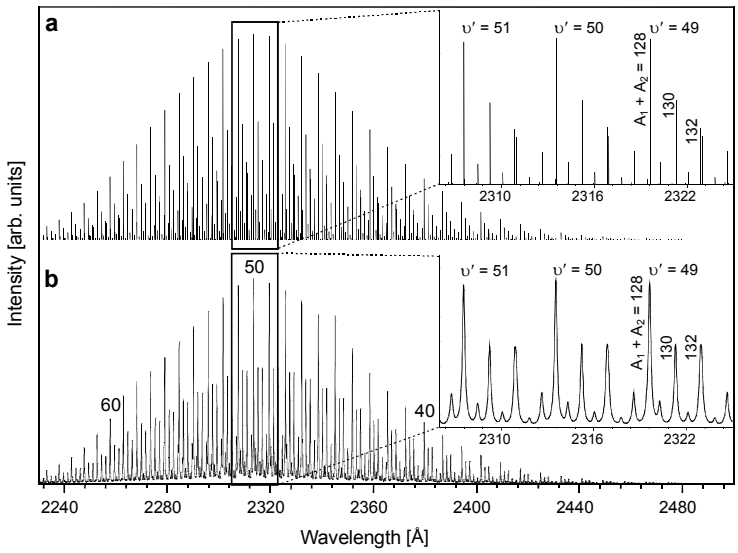

Fig. 2. Computer simulation of the excitation spectrum of the ${}^1 0^+_{u,\,\upsilon'}(4^1P_1) \leftarrow X^1 0^+_{g,\,\upsilon''=0}$ transition in Zn_2. To calculate energies of υ' and F–CFs for the $\upsilon' \leftarrow \upsilon'' = 0$ vibrational components a LEVEL 7.7 code [10] was employed. Three of the components with the largest intensity (the isotopic structure resulting from the natural abundance of Zn is included) are enlarged in the insert. The $(A_1 + A_2)$ values corresponding to the individual isotopic components are shown. The F–CFs for the total spectrum including the isotopic composition – **a**. Each of the isotopic components from (**a**) convoluted with a Lorentz function (FWHM = 0.2 Å) – **b**. The rotational structure was not taken into account.

bound and quasibound vibrational levels, the code can also calculate, *e.g.*, vibrational and rotational constants, vibrational wave functions and other properties of ro-vibration levels. Using the obtained results and an anharmonic oscillator approximation [15], we calculated the isotopic shifts for each of the $\upsilon' \leftarrow \upsilon'' = 0$ components according to the formula [13]

$$\Delta\nu_{ij}(\upsilon',\,\upsilon''=0) \;=\; (1-\rho)\left[\omega'_e\left(\upsilon'+\frac{1}{2}\right)-\frac{\omega''_e}{2}\right]-\left(1-\rho^2\right)\left[\omega'_e x'_e\left(\upsilon'+\frac{1}{2}\right)^2-\frac{\omega''_e\,x''_e}{4}\right] \tag{1}$$

where $\rho = \sqrt{\mu_i / \mu_j}$, μ_i and μ_j are the reduced masses of two Zn_2 isotopomers with different $(m_1 + m_2)$ mass combinations. At this stage of the simulation the rotational structure was not taken into account. However, to show its influence on the excitation spectrum, we simulated the rotational profile for one of the isotopic components. For this purpose, we chose $\upsilon' = 50$, *i.e.*, the vibrational component with the highest F–CF (see Figs. 2 and 3). The calculations of the rotational structure were carried out using

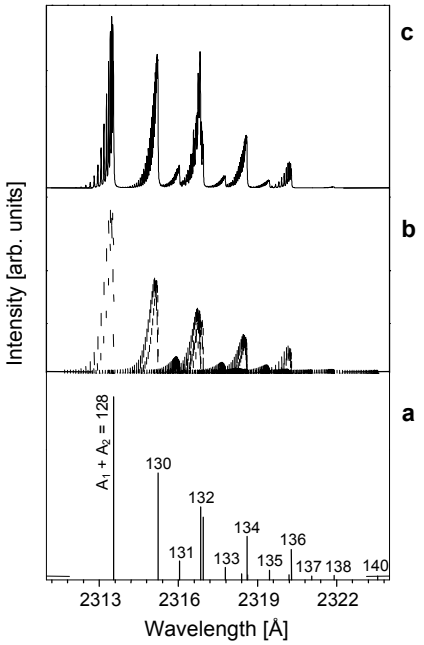

Fig. 3. Computer simulation of a rotational structure of the $\upsilon' = 50$ component from Fig. 2. Vertical lines representing amplitudes of all individual isotopic components with different mass combinations $(m_1 + m_2)$ within each of the $(A_1 + A_2)$ isotopic peaks showing a complex structure of vibrational components – **a**. Nuclear-spin intensity alternations and rotational-levels symmetry properties (*e.g.*, ref. [6]) of the total wave-function taken into account in simulations of *P* (short bars) and *R* (long bars) branches (*Q*-branch is not present [17]); rotational constants $B_{\upsilon'=50} = 0.063$ cm^{-1} and $B_{\upsilon''=0} = 0.030$ cm^{-1} were calculated from the equilibrium internuclear separations R'_e and R''_e, respectively obtained from *ab initio* calculation – **b**. A profile of the $\upsilon' = 50$ component obtained as a result of convolution of every rotational component with Lorentz function (FWHM = 0.016 Å) – **c**.

non-rigid rotator and anharmonic oscillator approximations [15, 17]. Consequently, the $\Delta\nu_P$ and $\Delta\nu_R$ frequency separations between energies of the rotational transitions for successive J (=J'') quantum numbers can be expressed by [13]

$$\Delta\nu_P = 2\left(B_{\upsilon'} - B_{\upsilon''}\right)J - 2B_{\upsilon''} \tag{2a}$$

$$\Delta\nu_R = 2\left(B_{\upsilon'} - B_{\upsilon''}\right)J + 2\left(2B_{\upsilon'} - B_{\upsilon''}\right) \tag{2b}$$

and corresponding $I(\nu_P)$ and $I(\nu_R)$, *i.e.*, *P*- and *R*-branch intensities (*Q*-branch is not present in the transition) can be expressed by the following relationships [15]:

$$I(\nu_P) \propto 2J\nu_P \exp\left[-\frac{B_{\upsilon''}J(J+1)hc}{kT_{\mathrm{rot}}}\right] \tag{3a}$$

$$I(\nu_R) \propto 2(J+1)\,\nu_R \exp\left[-\frac{B_{\upsilon''}J(J+1)hc}{kT_{\mathrm{rot}}}\right] \tag{3b}$$

where k and T_{rot} are the Boltzmann constant and rotational temperature, respectively. Rotational B_υ constants for vibrational components are given by [13]

$$B_\upsilon \approx B_e\left[1-\left(\upsilon+\frac{1}{2}\right)\frac{\omega_e x_e}{\omega_e}\right] \tag{4}$$

where $B_e = h/\left(8\pi^2 c\mu_r R_e^2\right)$, ω_e, $\omega_e x_e$ and μ_r are vibrational frequency, anharmonicity and reduced mass of a molecular isotopomer, respectively. The nuclear-spin intensity alternation as well as J-number symmetry properties of a total wave function were taken into account at this level of simulations. The idea of an analysis is presented in ref. [6].

3.2. Fluorescence spectrum of the $^1 0_u^+(4^1P_1) \rightarrow X^1 0_g^+$ transition

Similarly to the simulations presented above, we have used *ab initio* calculated points for the respective interatomic potentials in order to simulate a fluorescence spectrum of the $^1 0_u^+(4^1P_1)_{\upsilon'=50} \rightarrow X^1 0_g^+$ transition. The spectrum arises after a selective excitation of the $\upsilon' = 50$ level and the decay of the fluorescence on both, repulsive (free ← bound

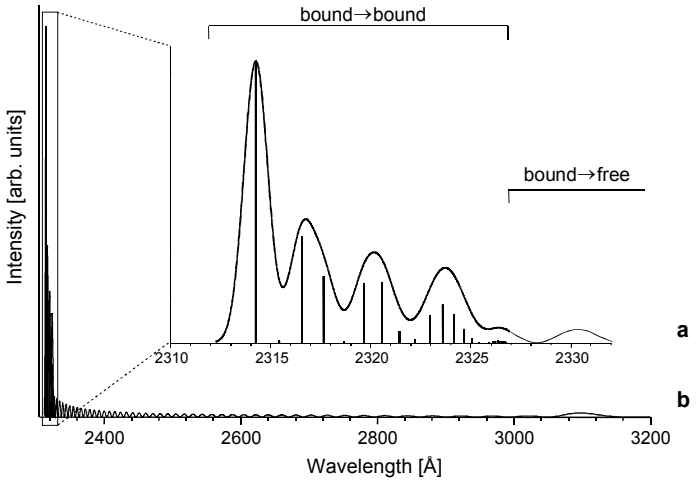

Fig. 4. Computer simulation of the fluorescence spectrum of the $^1 0_u^+(4^1P_1)_{\upsilon'=50} \rightarrow X^1 0_g^+$ transition in Zn_2. Simulation was performed using *ab initio* points calculated in this work. Short-wavelength part of the spectrum (bound → bound transitions) obtained using a LEVEL 7.7 code [10] – **a**, and long-wavelength part of the spectrum (bound → free transitions) obtained using a BCONT 2.2 code [11] – **b**. An envelope was obtained as a result of convolution of a Gaussian function (FWHM = 1.2 Å) with each of the vertical bars that correspond to F–CFs of the transition.

transitions) and bound parts (bound ← bound transitions) of the ground-state potential. Consequently, we had to divide the simulation into two parts using both LEVEL 7.7 [10] and BCONT 2.2 [11] codes. The results are shown in Fig. 4. A short-wavelength part of the spectrum consists of $\upsilon' = 50 \rightarrow \upsilon''$ bound → bound transitions (F–CFs), each represented with a vertical bar (see Fig. 4**a**). The F–CFs were convoluted with a Gaussian function that corresponds to a monochromator instrumental function. A long-wavelength part of the spectrum (Fig. 4**b**) represents an undulated structure corresponding to bound → free transitions from the $\upsilon' = 50$ directly to the repulsive part of the $X^1 0_g^+$-state potential. The number of maxima in both parts of the spectrum is equal to $\upsilon' + 1$ and can be used in an experiment to determine the υ' quantum number of the level from which the fluorescence is emitted.

4. Conclusions

The experimental and theoretical studies of Cd_2 and Zn_2 molecules are presented. Concerning the spectroscopy of Cd_2, the first attempt of detection of a laser induced fluorescence (LIF) after excitation of the Cd_2 from the $X^1 0_g^+$ to the higher-lying electronic states correlated with the 5^1P_1, 6^3S_1 and 6^1S_0 atomic asymptotes is reported. However, there are two articles of Grycuk and co-workers [18, 19] which investigated transitions between the three higher and $31_g(5^3P_1)$ electronic states in Cd_2. At this stage of the analysis it is concluded that the observed bound ← bound and free ← bound transitions are due to the excitation of the $^1 1_u(5^1P_1)$ electronic energy state. As regards the Zn_2, simulations comprising calculation of the vibrational energy states and corresponding F–CFs for the bound ← bound and free ← bound transitions of the $^1 0_u^+(4^1P_1)$–$X^1 0_g^+$ electronic transition are presented. The simulations of the spectra were made for two fundamental reasons. Firstly, as a test of the experimental approach and theoretical models describing behaviour of the dimers as well as their spectra. Secondly, they help to plan the future measurements. Neither of the simulations of the excitation and fluorescence spectra did take into account $M(R)$ transition moment for the transition under investigation.

References

[1] KOWALSKI A., CZAJKOWSKI M., BRECKENRIDGE W.H., *Laser excitation spectrum of the* $0_g^+(X^1\Sigma_g^+) - 0_u^+(^3\Pi_u)$ *transition in* Cd_2, Chemical Physics Letters **119**(4), 1985, pp. 368–70.

[2] CZAJKOWSKI M., BOBKOWSKI R., KRAUSE L., $0_u^+(^3\Pi_u) \leftarrow X0_g^+(\Sigma_g^+)$ *transitions in* Cd_2 *excited in crossed molecular and laser beams*, Physical Review A **40**(8), 1989, pp. 4338–43.

[3] CZAJKOWSKI M., KOPERSKI J., *The* Cd_2 *and* Zn_2 *van der Waals dimers revisited. Correction for some molecular potential parameters*, Spectrochimica Acta Part A: Molecular and Biomolecular Spectroscopy **55**(11), 1999, pp. 2221–9.

[4] KOPERSKI J., ŁUKOMSKI M., CZAJKOWSKI M., *Laser excitation spectrum and spectroscopic potential parameters of* Cd_2 *molecule in the* $1_u(5^3P_2)$ *energy state*, Spectrochimica Acta Part A: Molecular and Biomolecular Spectroscopy **58**(5), 2002, pp. 927–32.

[5] ŁUKOMSKI M., KOPERSKI J., CZUCHAJ E., CZAJKOWSKI M., *Structure of excitation and fluorescence spectra recorded at the $^1 0_u^+(5^1P_1) - X\,^1 0_g^+$ transition of Cd_2*, Physical Review A **68**(4), 2003, 042508; Erratum: Phys. Rev. A **69**, 2004, 049901(E).

[6] ŁUKOMSKI M., KOPERSKI J., *Nuclear-spin intensity alternation and rotational-levels symmetry properties in isotopically-resolved excitation spectrum of Cd_2*, Chemical Physics Letters **384**(4–6), 2004, pp. 317–9.

[7] ŁUKOMSKI M., RUSZCZAK M., CZUCHAJ E., KOPERSKI J., *Evidence of a weak dipole transition moment between the $X\,^1 0_g^+$ and $^3 1_u(5^3P_1)$ electronic energy states in Cd_2*, Spectrochimica Acta Part A: Molecular and Biomolecular Spectroscopy **61**(8), 2005, pp. 1835–40.

[8] CZAJKOWSKI M., BOBKOWSKI R., KRAUSE L., *$0_u^+(^3\Pi_u) \leftarrow X\,0_g^+(^1\Sigma_g^+)$ transitions in Zn_2 excited in crossed molecular and laser beams*, Physical Review A **41**(1), 1990, pp. 277–82.

[9] STROJECKI M., RUSZCZAK M., KROŚNICKI M., ŁUKOMSKI M., KOPERSKI J., *The $^3 0_u^+(4^3P_1)$-state potential of Zn_2 obtained from excitation spectrum recorded at the $^3 0_u^+ \leftarrow X\,^1 0_g^+$ transition*, Chemical Physics **327**(2–3), 2006, pp. 229–36.

[10] LEROY R.J., LEVEL 7.7, University of Waterloo Chemical Physics Research; Report CP-661, 2005. The source code http://leroy.uwaterloo.ca.

[11] LEROY R.J., KRAEMER G.T., BCONT 2.2, University of Waterloo Chemical Physics, Research Report CP-650R^2, 2004. The source code: http://leroy.uwaterloo.ca.

[12] WERNER H.-J., KNOWLES P.J., LINDH R., SCHÜTZ M., CELANI P., KORONA T., MANBY F.R., RAUHUT G., AMOS R.D., BERNHARDSSON A., BERNING A., COOPER D.L., DEEGAN M.J.O., DOBBYN A.J., ECKERT F., HAMPEL C., HETZER G., LLOYD A.W., MCNICHOLAS S.J., MEYER W., MURA M.E., NICKLASS A., PALMIERI P., PITZER R., SCHUMANN U., STOLL H., STONE A.J., TARRONI R., THORSTEINSSON T., MOLPRO, version 2002.6, a package of *ab initio* programs, 2003; see http://www.molpro.net.

[13] KOPERSKI J., *Study of diatomic van der Waals complexes in supersonic beams*, Physics Reports **369**(3), 2002, pp. 177–326.

[14] RUSZCZAK M., STROJECKI M., KOPERSKI J., *Short-range repulsion in the $D^1 0^+(^1\Sigma^+)$-state potential of the CdRG (RG = Ar, Kr) molecules determined from a direct continuum $\leftarrow$ bound excitation detected at the $D^1 0^+ \leftarrow X^1 0^+(^1\Sigma^+)$ transition*, Chemical Physics Letters **416**(1–3), 2005, pp. 147–51.

[15] HERZBERG G., *Molecular Spectra and Molecular Structure. I. Spectra of Diatomic Molecules*, D. Van Nostrand, Princeton, New Jersey 1950.

[16] CZUCHAJ E., private communication, 2005.

[17] BROWN J.M., CARRINGTON A., *Rotational Spectroscopy of Diatomic Molecules*, 1st Edition, Cambridge University Press, Cambridge 2003.

[18] KUTNER T., DAGLEWICZ-NOWAK R., GRYCUK T., *Fluorescence spectra of the Cd_2 dimer: transitions involving 0_u^+ and 1_u Rydberg states and the lowest excited gerade states*, Chemical Physics Letters **384**(1–3), 2004, pp. 171–8.

[19] KUTNER T., KUBKOWSKA M. K., GRYCUK T., *Absorption and emission studies of the $0_g^+(5^1S_0)$–$1_u(6^3S_1)$ transition in the Cd dimer*, Journal of Molecular Spectroscopy **233**(1), 2005, pp. 149–56.

Received January 30, 2006
in revised form April 21, 2006